nature structural & molecular biology

SUPPLEMENTARY INFORMATION

https://doi.org/10.1038/s41594-018-0116-7

In the format provided by the authors and unedited.

Structural determinants of 5-HT_{2B} receptor activation and biased agonism

John D. McCorvy[1,3,6*], Daniel Wacker[1,4,6], Sheng Wang[1,5,6], Bemnat Agegnehu[1], Jing Liu[2], Katherine Lansu[1], Alexandra R. Tribo[1], Reid H. J. Olsen[1], Tao Che[1], Jian Jin[2] and Bryan L. Roth[1*]

[1]National Institute of Mental Health Psychoactive Drug Screening Program, Department of Pharmacology and Division of Chemical Biology and Medicinal Chemistry, University of North Carolina Chapel Hill Medical School, Chapel Hill, NC, USA. [2]Center for Chemical Biology and Drug Discovery, Department of Pharmacological Sciences and Department of Oncological Sciences, Tisch Cancer Institute, Icahn School of Medicine at Mount Sinai, New York, NY, USA. [3]Present address: Department of Cell Biology, Neurobiology and Anatomy, Medical College of Wisconsin, Milwaukee, WI, USA. [4]Present address: Department of Pharmacological Sciences and Department of Neuroscience, Icahn School of Medicine at Mount Sinai, New York, NY, USA. [5]Present address: State Key Laboratory of Molecular Biology, Institute of Biochemistry and Cell Biology, Shanghai Institutes for Biological Sciences, Chinese Academy of Sciences, Shanghai, China. [6]These authors contributed equally: John D. McCorvy, Daniel Wacker, Sheng Wang. *e-mail: jmccorvy@mcw.edu; bryan_roth@med.unc.edu

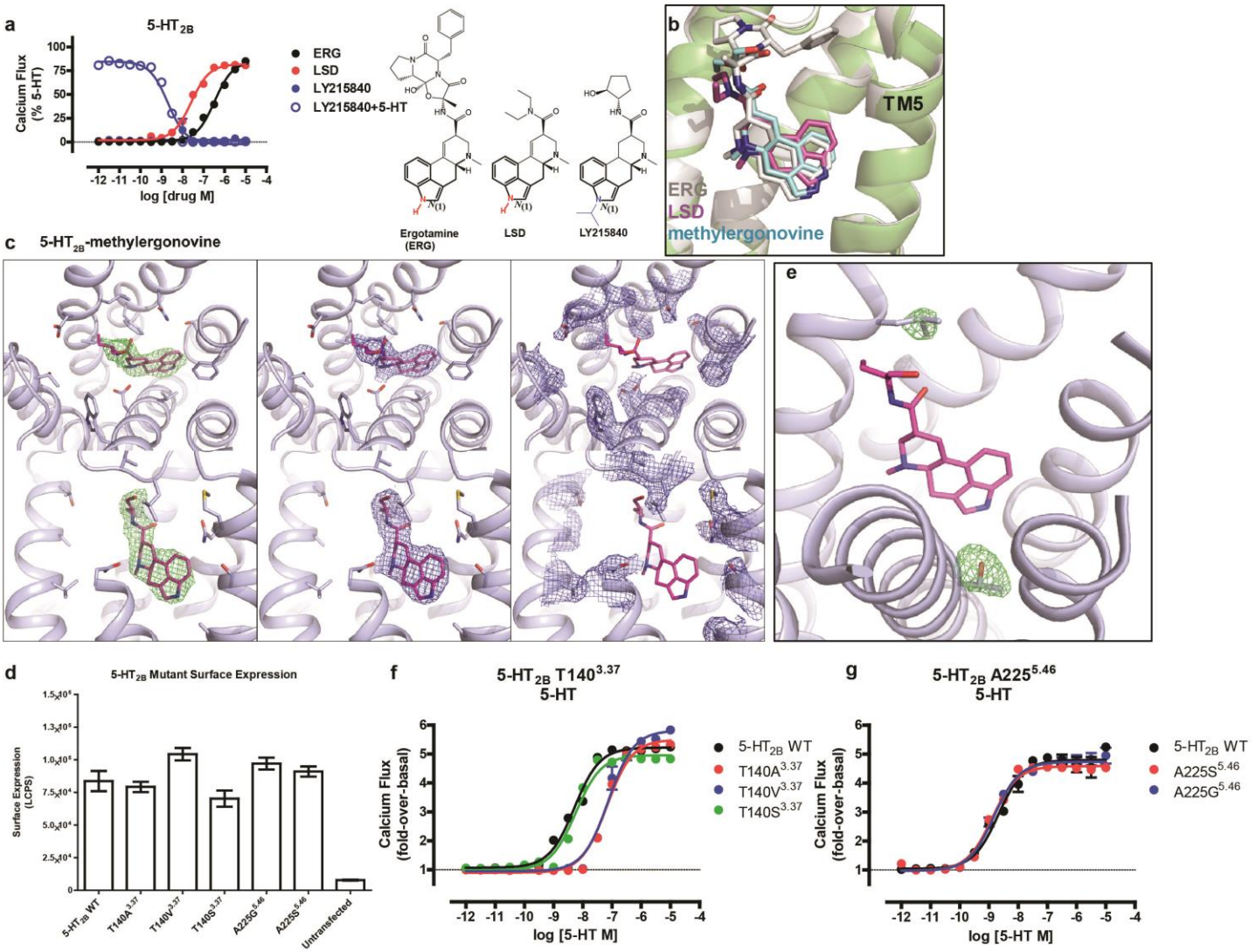

Supplementary Figure 1

Activation mechanisms and 5-HT$_{2B}$R–methylergonovine structure.

a, Additional 5-HT$_{2B}$R ergoline SAR showing G_q-mediated calcium flux by *N*(1)-H-containing ergolines, LSD (red, EC_{50} = 26 nM, E_{max} = 82%) and ergotamine (ERG, black, EC_{50} = 334 nM, E_{max} = 85%) and antagonism by *N*(1)-alkyl ergolines, including LY215840, which contains *N*(1)-isopropyl (blue, IC_{50}= 2.0 nM). Data are expressed as percent 5-HT response and represent means ± s.e.m. from two independent experiments (*n* = 2) performed in triplicate. **b**, Alignment of the 5-HT$_{2B}$R ERG (gray), LSD (purple) and methylergonovine (light blue) crystal structures reveals slight differences in positioning of the indole *N*(1)-H with respect to TM5. **c**, 5-HT$_{2B}$R–methylergonovine structure $F_o - F_c$ omit map of ligand (left), $2F_o - F_c$ regular map of ligand (middle) and binding pocket residues (right). **d**, Surface expression measured by ELISA reveals similar expression levels of the T140$^{3.37}$ and A225$^{5.46}$ mutants as for wild-type 5-HT$_{2B}$R. Data represent means ± s.e.m. from quadruplicate replicates from two independent experiments (*n* = 2). **e**, $F_o - F_c$ omit density map of residues T140$^{3.37}$ and L362$^{7.35}$ in the 5-HT$_{2B}$R–methylergonovine structure. **f**, 5-HT G_q-mediated calcium flux agonist potency at T140A$^{3.37}$ (red, EC_{50} = 73 nM) and T140V$^{3.37}$ (blue, EC_{50} = 93 nM) compared to T140S$^{3.37}$ (green, EC_{50} = 5.7 nM) and wild-type 5-HT$_{2B}$R (black, EC_{50} = 5.2 nM). Data are expressed as fold-over-basal and represent means ± s.e.m. from two independent experiments (*n* = 2) performed in triplicate. **g**, 5-HT G_q-mediated calcium flux agonist potency at A225S$^{5.46}$ (red, EC_{50} = 1.4 nM) and A225G$^{5.46}$ (blue, EC_{50} = 1.5 nM) as compared to wild-type 5-HT$_{2B}$R (black, EC_{50} = 3.2 nM). Data are expressed as fold-over-basal and represent means ± s.e.m. from two independent experiments (*n* = 2) performed in triplicate.

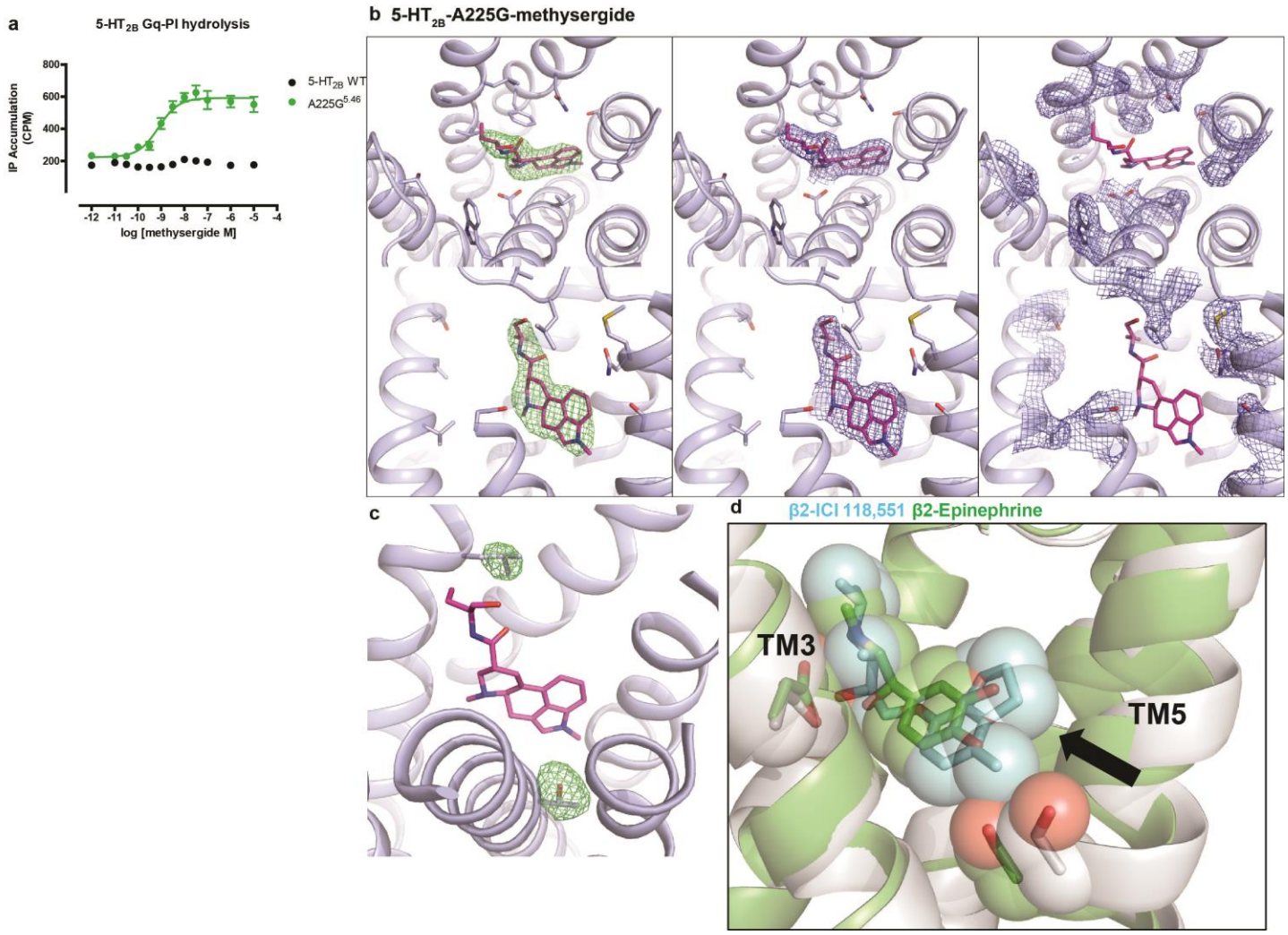

Supplementary Figure 2

Activation mechanism and 5-HT$_{2B}$R(A225G$^{5.46}$)–methysergide structure.

a, 5-HT$_{2B}$R G_q-mediated PI hydrolysis showing similar basal levels of IP accumulation and G_q agonist activity by methysergide for A225G$^{5.46}$ (green, EC_{50} = 0.7 nM) compared to no measured agonist activity for wild-type 5-HT$_{2B}$R (black). Data are expressed as counts per minute (CPM) of [^{3}H]IP and represent means ± s.e.m. from three independent experiments (n = 3) performed in duplicate. **b**, 5-HT$_{2B}$R(A225G$^{5.46}$)–methysergide structure F_o – F_c omit map of ligand (left), 2F_o – F_c regular map of ligand (middle) and binding pocket residues (right). **c**, F_o – F_c omit density map of residues T140$^{3.37}$ and L362$^{7.35}$ in the 5-HT$_{2B}$R(A225G$^{5.46}$)–methysergide structure. **d**, Alignment of the structure for the β_2AR–ICI-118,551 complex (blue) with the nanobody-stabilized active state of β_2AR in complex with epinephrine (green) indicates that the methyl of ICI-118,551 precludes inward TM5 movement.

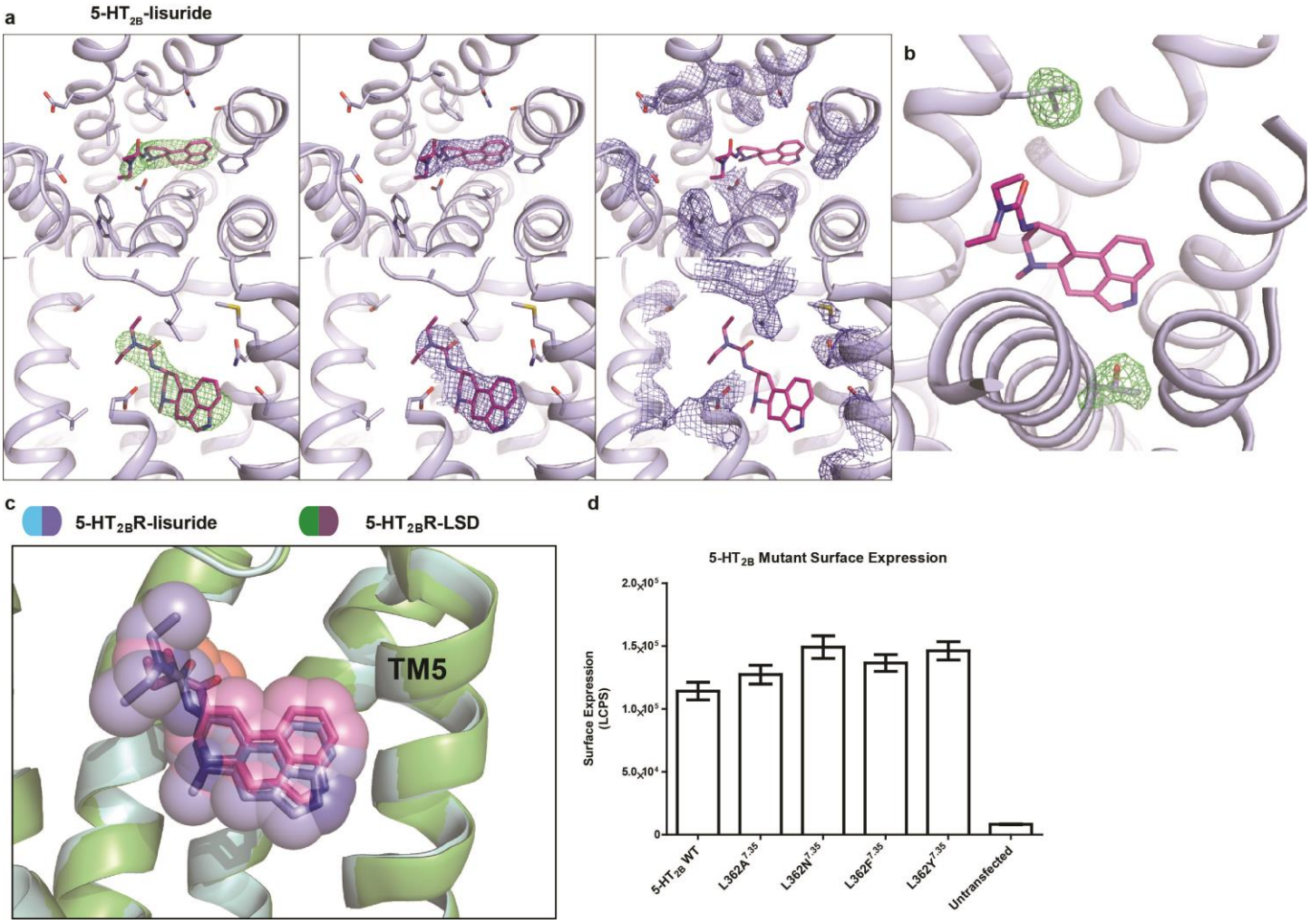

Supplementary Figure 3

5-HT$_{2B}$R–lisuride structure and OBP mutant L362$^{7.35}$ surface expression.

a, 5-HT$_{2B}$R–lisuride structure $F_o - F_c$ omit map of ligand (left), $2F_o - F_c$ regular map of ligand (middle) and binding pocket residues (right). **b**, $F_o - F_c$ omit density map of residues T140$^{3.37}$ and L362$^{7.35}$ in the structure of lisuride-bound 5-HT$_{2B}$R. **c**, Alignment of the structures for the 5-HT$_{2B}$R–LSD and 5-HT$_{2B}$R–lisuride complexes reveals similar positioning of the indole *N*(1)-H with respect to TM5. **d**, Surface expression measured by ELISA reveals similar expression levels of L362$^{7.35}$ mutants as for wild-type 5-HT$_{2B}$R. Data represent means ± s.e.m. from quadruplicate replicates from two independent experiments (n = 2).

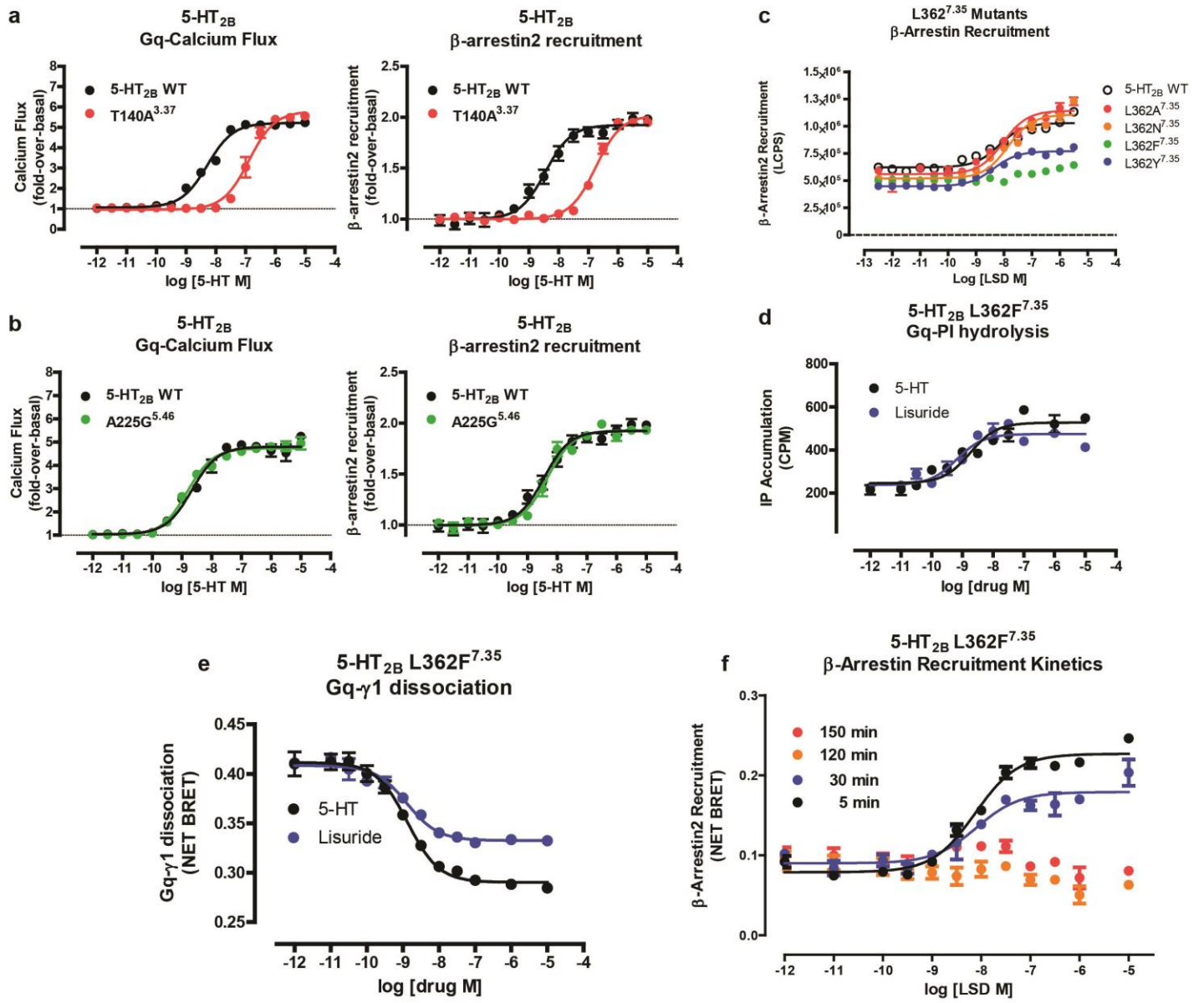

Supplementary Figure 4

Divergent function by OBP versus EBP mutations.

a, Left, 5-HT G_q-mediated calcium flux comparing T140A$^{3.37}$ (red, EC_{50} = 130 nM) to wild-type 5-HT_{2B}R (black, EC_{50} = 5.2 nM). Right, 5-HT β-arrestin2 recruitment comparing T140A$^{3.37}$ (red, EC_{50} = 178 nM) to wild-type 5-HT_{2B}R (black, EC_{50} = 3.6 nM). **b**, Left, 5-HT G_q-mediated calcium flux comparing A225G$^{5.46}$ (green, EC_{50} = 1.5 nM) to wild-type 5-HT_{2B}R (black, EC_{50} = 2.2 nM). Right, 5-HT β-arrestin2 recruitment comparing A225G$^{5.46}$ (green, EC_{50} = 4.6 nM) to wild-type 5-HT_{2B}R (black, EC_{50} = 3.6 nM). Data in **a** and **b** are expressed as fold-over-basal and represent means ± s.e.m. from two independent experiments (n = 2) performed in triplicate. **c**, LSD β-arrestin2 recruitment for the L362A$^{7.35}$ (red), L362N$^{7.35}$ (orange), L362Y$^{7.35}$ (blue) and L362F$^{7.35}$ (green) 5-HT_{2B}R mutants. Data are expressed as luminescent counts per second (LCPS), indicating β-arrestin2 recruitment as measured by Tango, and represent means ± s.e.m. from two independent experiments (n = 2) performed in triplicate. **d**, Mutant 5-HT_{2B}R L362F$^{7.35}$ G_q-mediated PI hydrolysis by 5-HT (black, EC_{50} = 1.8 nM) and lisuride (blue, EC_{50} = 0.65 nM). Data are expressed as counts per minute (CPM) of [^{3}H]IP and represent means ± s.e.m. from two independent experiments (n = 2) performed in duplicate. **e**, Mutant 5-HT_{2B}R L362F$^{7.35}$ $G_{q/\gamma 1}$ dissociation as measured by BRET[2] showing 5-HT (black, EC_{50} = 1.3 nM) and lisuride (blue, EC_{50} = 1.2 nM) G_q agonist activity. Data are represented as means ± s.e.m. from two independent experiments (n = 2) and are expressed as NET BRET ratio (Methods). **f**, Mutant 5-HT_{2B}R L362F$^{7.35}$ LSD β-arrestin2 recruitment as measured by BRET[1]. Data are represented as means ± s.e.m. from two independent experiments (n = 2) and are expressed as NET BRET ratio (Methods).

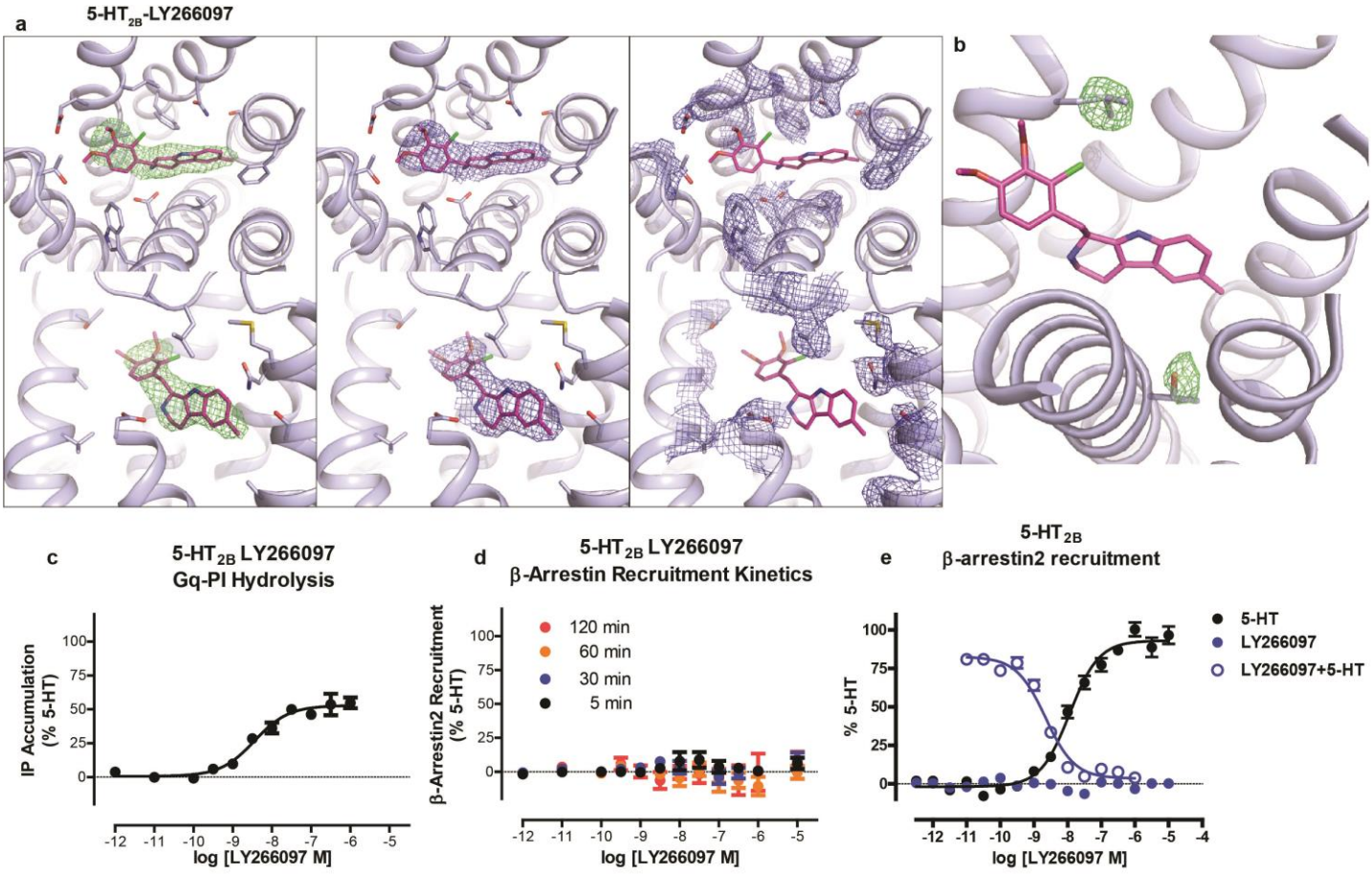

Supplementary Figure 5

5-HT$_{2B}$R structure and function by LY266097.

a, 5-HT$_{2B}$R–LY266097 structure $F_o - F_c$ omit map of ligand (left), $2F_o - F_c$ regular map of ligand (middle) and binding pocket residues (right). **b**, $F_o - F_c$ omit density map of residues T140$^{3.37}$ and L362$^{7.35}$ in the 5-HT$_{2B}$R–LY266097 structure. **c**, LY266097 5-HT$_{2B}$R G_q-mediated PI hydrolysis (EC_{50} = 3.6 nM, E_{max} = 52%). Data are expressed as percent 5-HT response and represent means ± s.e.m. from three independent experiments (n = 3) performed in duplicate. **d**, LY266097 β-arrestin2 recruitment as measured by BRET[1] over 5, 30, 60 and 120 min. Data represent means ± s.e.m. from two independent experiments (n = 2) performed in duplicate and are expressed as percent 5-HT NET BRET ratio response. **e**, β-arrestin2 recruitment as measured by Tango comparing agonist activity of 5-HT (black, EC_{50} = 11 nM) to LY266097 (blue, closed circles), where LY266097 exhibits β-arrestin2 recruitment antagonism (blue, open circles, IC_{50} = 2.2 nM) of 5-HT. Data represent means ± s.e.m. from two independent experiments (n = 2) performed in triplicate and are expressed as percent 5-HT response.

Supplementary Table 1. 5-HT_{2B} Mutant Affinity Table

Data represent average Kd/Ki and average pKd/pKi ± S.E.M. from three independent experiments performed in duplicate and were acquired with 5-HT_{2B} wild-type and mutants expressed in HEK cells. Affinity was assessed by radioligand competition binding performed using [^{3}H]-LSD (0.2 -0.7 nM) to yield Kd or Ki affinity estimates. The pKd and pKi values were compared using a one-way ANOVA with Dunnett's post-test comparing mutant to WT (** = p<0.01).

5-HT_{2B} Mutant	**LSD**		**methylergonovine**		**methysergide**	
	Kd, nM (pKd ±SEM)	**ΔpKd (mutant - WT)**	**Ki, nM (pKi ±SEM)**	**ΔpKi (mutant - WT)**	**Ki, nM (pKi ±SEM)**	**ΔpKi (mutant - WT)**
5-HT_{2B} WT	0.58 (9.33±0.14)	---	0.37 (9.48±0.11)	---	0.16 (9.83±0.08)	---
T140A$^{3.37}$	1.41 (8.93±0.16)	-0.39	4.18** (8.40±0.08)	-0.93	0.39 (9.59±0.09)	-0.25
T140V$^{3.37}$	1.33 (8.99±0.18)	-0.34	8.03** (8.15±0.13)	+1.33	0.30 (9.63±0.16)	-0.20
T140S$^{3.37}$	0.75 (9.13±0.08)	-0.19	0.51 (9.30±0.08)	-0.18	0.25 (9.60±0.07)	-0.23
A225S$^{5.46}$	0.28 (9.74±0.23)	+0.42	0.30 (9.59±0.19)	+0.11	1.77** (8.98±0.26)	-0.85
A225G$^{5.46}$	1.31 (8.89±0.04)	-0.44	0.96 (9.02±0.03)	-0.46	0.24 (9.62±0.02)	-0.21

Supplementary Note 1: Synthetic Chemistry Procedures

All of the compounds were prepared according to known synthetic procedures[1,2].

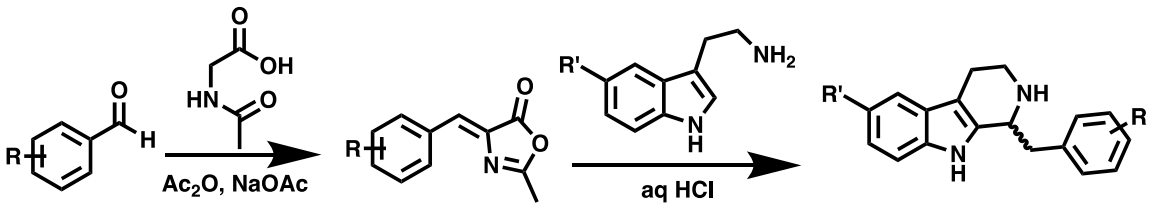

General procedures for the preparation of aza lactones. To a solution of substituted benzaldehyde (1.0 mmol) in 2 mL acetic anhydride was added *N*-acetylglycine (1.0 mmol) followed by sodium acetate (1.0 mmol). The reaction mixture was heated at 100 °C for 4 h before being cooled down to rt for overnight. The resulting precipitate was filtered, washed with cold diethyl ether, and dried under vacuum. The crude aza lactone was used for the next step without further purification.

General procedures for the condensation of aza lactones with tryptamines. To a solution of typtamine hydrochloride (0.26 mmol) in 1 M aqueous hydrochloric acid (4 mL) was added the crude aza lactone (0.4 mmol). The mixture was heated at 100 °C for 36 h. After being cooled to room temperature, the reaction was quenched with saturated sodium bicarbonate aqueous solution and diluted with ethyl acetate. After the separation of the two layers, the aqueous layer was extracted with ethyl acetate 3 times. The combined organic layers were dried over sodium sulfate and concentrated. The resulting residue was purified by silica gel chromatography to provide the desired product.

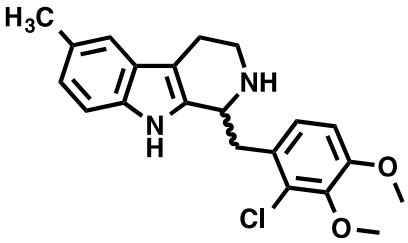

1-(2-Chloro-3,4-dimethoxybenzyl)-6-methyl-2,3,4,9-tetrahydro-1*H*-pyrido[3,4-*b*]indole (LY266097). (58% yield) Enantiomer **1**. ^{1}H NMR (600 MHz, CD_3OD) δ 7.54 (s, 1H), 7.28 (s, 1H), 7.18 (d, *J* = 8.2 Hz, 1H), 7.02 (d, *J* = 8.4 Hz, 1H), 6.97 (dd, *J* = 8.2, 1.6 Hz, 1H), 6.82 (d, *J* = 8.5 Hz, 1H),

4.41 – 4.35 (m, 1H), 3.90 (s, 3H), 3.89 (s, 3H), 3.36 – 3.24 (m, 2H), 3.05 (ddd, *J* = 12.4, 7.2, 4.9 Hz, 1H), 2.96 (dd, *J* = 13.8, 8.6 Hz, 1H), 2.81 – 2.74 (m, 1H), 2.71 (dtd, *J* = 15.3, 5.2, 1.6 Hz, 1H), 2.44 (s, 3H), 1.66 (s, overlap with H_2O peak, 1H). HRMS calcd. for $C_{21}H_{23}ClN_2O_2$ + H: 371.1526; found: 371.1524 $[M + H]^+$. Enantiomer **2**. ^1H NMR (600 MHz, CD_3OD) δ 7.53 (s, 1H), 7.28 (d, *J* = 1.6 Hz, 1H), 7.18 (d, *J* = 8.1 Hz, 1H), 7.02 (d, *J* = 8.4 Hz, 1H), 6.97 (dd, *J* = 8.2, 1.6 Hz, 1H), 6.82 (d, *J* = 8.5 Hz, 1H), 4.40 – 4.34 (m, 1H), 3.90 (s, 3H), 3.89 (s, 3H), 3.35 – 3.25 (m, 2H), 3.09 – 3.01 (m, 1H), 2.96 (dd, *J* = 13.7, 8.7 Hz, 1H), 2.81 – 2.74 (m, 1H), 2.74 – 2.67 (m, 1H), 2.44 (s, 3H), 1.62 (s, overlap with H_2O peak, 1H). HRMS calcd. for $C_{21}H_{23}ClN_2O_2$ + H: 371.1526; found: 371.1525 $[M + H]^+$.

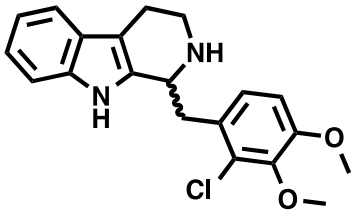

1-(2-Chloro-3,4-dimethoxybenzyl)-2,3,4,9-tetrahydro-1*H*-pyrido[3,4-*b*]indole. (55% yield) ^1H NMR (600 MHz, $CDCl_3$) δ 7.67 (s, 1H), 7.50 (d, *J* = 7.7 Hz, 1H), 7.29 (d, *J* = 8.0 Hz, 1H), 7.15 (dd, *J* = 8.1, 6.9 Hz, 1H), 7.12 – 7.07 (m, 1H), 7.03 (d, *J* = 8.4 Hz, 1H), 6.82 (d, *J* = 8.4 Hz, 1H), 4.43 – 4.35 (m, 1H), 3.91 (s, 3H), 3.89 (s, 3H), 3.37 – 3.26 (m, 2H), 3.07 (ddd, *J* = 12.4, 7.2, 4.9 Hz, 1H), 2.98 (dd, *J* = 13.8, 8.7 Hz, 1H), 2.84 – 2.78 (m, 1H), 2.78 – 2.70 (m, 1H), 1.77 (s, 1H). HRMS calcd. for $C_{20}H_{21}ClN_2O_2$ + H: 357.1370; found: 357.1365 $[M + H]^+$.

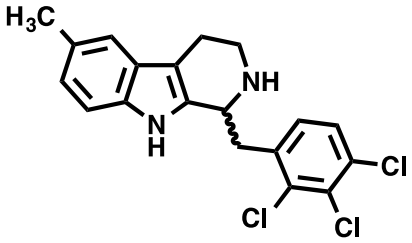

6-Methyl-1-(2,3,4-trichlorobenzyl)-2,3,4,9-tetrahydro-1*H*-pyrido[3,4-*b*]indole. (42% yield) ^1H NMR (600 MHz, $CDCl_3$) δ 7.58 (s, 1H), 7.36 (d, *J* = 8.3 Hz, 1H), 7.29 (s, 1H), 7.21 (d, *J* = 8.2 Hz, 1H), 7.19 (d, *J* = 8.3 Hz, 1H), 7.00 (dd, *J* = 8.3, 1.6 Hz, 1H), 4.41 – 4.34 (m, 1H), 3.36 (dd, *J* = 13.8, 4.5 Hz, 1H), 3.29 (dt, *J* = 12.8, 5.4 Hz, 1H), 3.06 (ddd, *J* = 12.4, 6.7, 5.0 Hz, 1H), 3.01 (dd, *J* = 13.8, 9.3 Hz, 1H),

2.81 – 2.74 (m, 1H), 2.74 – 2.66 (m, 1H), 2.45 (s, 3H), 1.64 (s, 1H). HRMS calcd. for $C_{19}H_{17}Cl_3N_2$ + H: 379.0536; found: 379.0532 $[M + H]^+$.

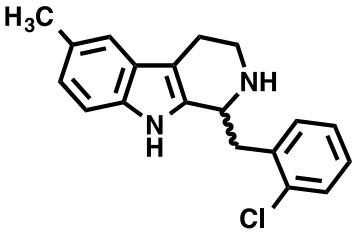

1-(2-Chlorobenzyl)-6-methyl-2,3,4,9-tetrahydro-1*H*-pyrido[3,4-*b*]indole. (38% yield) ^{1}H NMR (600 MHz, $CDCl_3$) δ 7.49 (s, 1H), 7.45 – 7.41 (m, 1H), 7.34 – 7.30 (m, 1H), 7.28 (s, 1H), 7.26 – 7.23 (m, 2H), 7.16 (d, *J* = 8.2 Hz, 1H), 6.97 (d, *J* = 8.2 Hz, 1H), 4.50 – 4.39 (m, 1H), 3.37 – 3.27 (m, 2H), 3.11 – 3.01 (m, 2H), 2.83 – 2.75 (m, 1H), 2.75 – 2.67 (m, 1H), 2.44 (s, 3H), 1.92 – 1.74 (m, 1H). HRMS calcd. for $C_{19}H_{19}ClN_2$ + H: 311.1315; found: 311.1318 $[M + H]^+$.

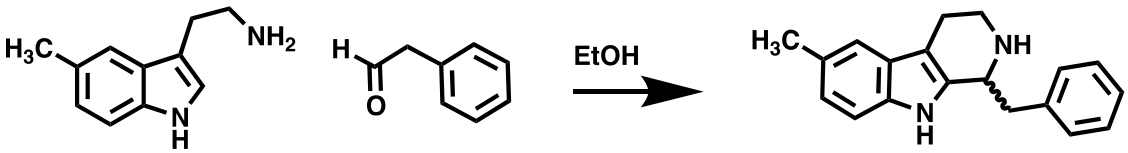

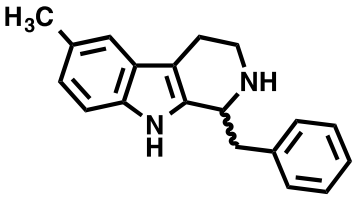

1-Benzyl-6-methyl-2,3,4,9-tetrahydro-1*H*-pyrido[3,4-*b*]indole. To a solution of 2-(5-methyl-1H-indol-3-yl)ethan-1-amine (0.063 g, 0.3 mmol) in ethanol (5 mL) was added phenylacetaldehyde (0.044 g, 0.36 mmol). The reaction was heated at 78 °C for 72 h before being cooled to rt and concentrated under reduced pressure. The residue was diluted with ethyl acetate and washed with saturated sodium bicarbonate aqueous solution. After the separation of the two layers, the aqueous layer was extracted with ethyl acetate 3 times. The combined organic layers were dried over sodium sulfate and concentrated. The resulting residue was purified by silica gel chromatography to provide the desired product (0.042 g, 51%). ^{1}H NMR (600 MHz, $CDCl_3$) δ 7.38 – 7.33 (m, 2H), 7.32 – 7.27 (m, 3H), 7.26

(s, 1H), 7.26 – 7.23 (m, 1H), 7.09 (d, *J* = 8.2 Hz, 1H), 6.95 (dd, *J* = 8.3, 1.6 Hz, 1H), 4.38 (t, *J* = 7.2 Hz, 1H), 3.33 (dt, *J* = 12.6, 4.9 Hz, 1H), 3.15 – 3.09 (m, 1H), 3.08 – 2.99 (m, 2H), 2.80 – 2.65 (m, 2H), 2.43 (s, 3H), 1.77 (s, 1H). HRMS calcd. for $C_{19}H_{20}N_2$ + H: 277.1705; found: 277.1708 $[M + H]^+$.

References

1. Audia, J.E., Droste, J.J., Nissen, J.S., Murdoch, G.L. & Evrard, D.A. "Pictet-Spengler-like" Synthesis of Tetrahydro-beta-carbolines under Hydrolytic Conditions. Direct Use of Azalactones as Phenylacetaldehyde Equivalents. *J Org Chem* **61**, 7937-7939 (1996).
2. Audia, J.E. et al. Potent, selective tetrahydro-beta-carboline antagonists of the serotonin 2B (5HT2B) contractile receptor in the rat stomach fundus. *J Med Chem* **39**, 2773-80 (1996).